ROTORDYNAMIC DESIGN OF CENTRIFUGAL COMPRESSORS IN ACCORDANCE WITH THE NEW API STABILITY SPECIFICATIONS

by
John C. Nicholas
Owner, Director, Chief Engineer
Rotating Machinery Technology, Inc.
Wellsville, New York
and
John A. Kocur
Machinery Engineer
ExxonMobil Research and Engineering Company
Fairfax, Virginia

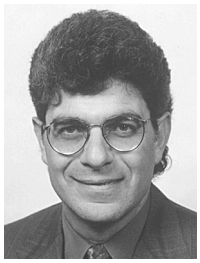

John C. Nicholas is the owner, Director, and Chief Engineer of Rotating Machinery Technology, Incorporated, a company that repairs and services turbomachinery, and manufactures bearings and seals. He has worked in the turbomachinery industry for 28 years in the rotor and bearing dynamics areas, including five years at Ingersoll-Rand and five years as the Supervisor of the Rotordynamics Group at the Steam Turbine Division of Dresser-Rand.

Dr. Nicholas, a member of ASME, STLE, and the Vibration Institute, has authored over 40 technical papers, concentrating his efforts on tilting pad journal bearing design and application. He received his B.S. degree from the University of Pittsburgh (Mechanical Engineering, 1968) and his Ph.D. degree from the University of Virginia (1977) in rotor and bearing dynamics. Dr. Nicholas holds several patents including one for a spray-bar blocker design for tilting pad journal bearings and another concerning bypass cooling technology for journal and thrust bearings.

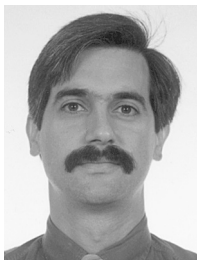

John A. Kocur, Jr., is a Machinery Engineer in the Plant Engineering Division at ExxonMobil Research & Engineering, in Fairfax, Virginia. He has worked in the turbomachinery field for 20 years. He provides support to the downstream business within ExxonMobil with expertise on vibrations, rotor/aerodynamics, and health monitoring of rotating equipment. Prior to joining EMRE, he held the position of Manager of Product Engineering and Testing at Siemens Demag Delaval Turbomachinery. There Dr. Kocur directed the development, research, engineering, and testing of compressor and steam turbine product lines.

Dr. Kocur received his BSME (1978), MSME (1982), and Ph.D. (1991) from the University of Virginia and an MBA (1981) from Tulane University. He has authored papers on rotor instability and bearing dynamics, lectured on hydrostatic bearings, has been a committee chairman for NASA Lewis, and is a member of ASME. Dr. Kocur holds a patent on angled supply injection of hydrostatic bearings.

ABSTRACT

The American Petroleum Institute (API) has recently implemented new rotordynamic stability specifications for centrifugal compressors. The specifications consist of a Level I analysis that approximates the destabilizing effects of the labyrinth seals and aerodynamic excitations. A modified Alford's equation is used to approximate the destabilizing effects. If the compressor fails the Level I specifications, a more sophisticated Level II analysis is required that includes a detailed labyrinth seal analysis.

Five modern high-pressure example centrifugal compressors are considered along with a classic instability case, Kaybob. After applying API Level I and Level II stability analyses and reviewing the results, design changes are made to stabilize the compressors, if necessary. For these cases, the API stability specifications are used to identify the component with the greatest impact on rotor stability. Specifically, the balance piston seal and impeller eye seals are analyzed. The suitability of applying the modified Alford's equation to compressors with multiple process stages is examined and compared to the full labyrinth seal analysis. Important aspects of labyrinth seal analyses are discussed, such as seal clearance effects, inlet swirl effects, and converging, diverging clearance effects. Finally, a modal approach to applying the labyrinth seal calculated cross-coupled forces is presented. For all five example compressors, the modified Alford's force was determined to produce the worst case stability level compared to labyrinth calculated forces.

INTRODUCTION

Centrifugal compressor instability became a major problem in the 1960s due to increased speeds and power ratings. Unstable compressors exhibited a high subsynchronous vibration whose vibration frequency coincided with the rotor's first fundamental natural frequency. Two famous and classic centrifugal compressor instability cases from the early 1970s are referred to as Kaybob (Smith, 1975; Fowlie and Miles, 1975) and Ekofisk (Geary, et al., 1976). Both problems occurred onsite and the solution involved a costly and time-consuming effort ultimately requiring rotor redesigns.

As a result of these experiences, the evaluation of rotor system stability has become an essential part of rotordynamic analyses and rotating machinery design. Most often, the lowest or first mode, corresponding to the rotor's first fundamental natural frequency, is the mode that is "reexcited" causing the subsynchronous vibration and rotor instability. The primary results of a stability or damped

natural frequency analysis are the stability prediction from the real part and the predicted instability frequency from the imaginary part of the solution roots or eigenvalues.

Some of the earliest stability work includes two classic publications by Gunter where basic stability methodology (Gunter, 1966) and internal friction excitation (Gunter, 1967) are discussed. Initial attempts at developing a stability computer code were made by Lund (1965). Lund's code was not easy to use and it was said that if one knew the approximate answer the code would converge on the solution. Another early computer code was by Ruhl and Booker (1972). They presented both finite element and transfer matrix solution techniques using a Muller's method solver. For lightly damped systems, their transfer matrix solution analysis worked fine but for more heavily damped structures, such as fluid film bearing supported turbomachinery, the program's analysis methodology produced incorrect and false modes.

These shortcomings were overcome in Lund's landmark stability paper (1974). Lund not only outlines a detailed transfer matrix solution procedure, but also describes how the stability results may be presented to study machine design parameters. His transfer matrix solution is able to search for the first several modes very efficiently, solving for the most important lowest frequency modes first, although in random order.

Ruhl's transfer matrix analysis was updated to include flexible supports by Bansal and Kirk (1975), replacing Muller's solver with a Cauchy-Rieman condition finite difference algorithm plus a Newton-Raphson search solution specified by Kirk (1980). With minor differences, this was essentially the same solution as used by Lund (1974). Both procedures work but will occasionally skip modes especially when asymmetric flexible supports are included at the bearing locations. Other transfer matrix computer programs have been developed based on Lund's original analysis such as Barrett, et al. (1976).

More recent computer codes are based on a finite element solution that successfully extracts all of the correct modes. These finite element code authors include Nelson and McVaugh (1975), Rouch and Kao (1979), Edney, et al. (1990), Chen (1996), and Ramesh and Kirk (1993). One disadvantage of the finite element analysis was that the problem size increases dramatically with the number of elements used to model the rotor, resulting in longer run times compared to the transfer matrix method. However, this is no longer an issue with the fast processing speed of modern personal computers. Additionally, some methods require that all roots be found, extracting the highest natural frequency first and ending with the lowest, most important mode. Alternate solution techniques are now available that extract the lowest eigenvalues first (Murphy and Vance, 1983).

The most recent API Standard 617, Seventh Edition (2002), for centrifugal compressors includes stability acceptance criteria along with analytical procedures. The stability specification is segmented into two parts: a simplified Level I analysis and a detailed Level II analysis. The Level I analysis is meant to be a screening process in which a quick and simple analysis can be conducted to filter out machines that are well away from the instability threshold. Level I utilizes a modified Alford's equation (Alford, 1965) to estimate the destabilizing forces. The Tutorial on Rotordynamics, API Technical Publication 684 (2005), presents a discussion of the modified Alford's equation. The more involved Level II analysis requires that the dynamic properties of labyrinth seals be included implicitly through the use of an appropriate labyrinth seal code. Initial labyrinth seal computer codes based on the Iwatsubo, et al. (1982), solution were developed by Childs and Scharrer (1986b). Kirk (1988a, 1988b, 1990) further extended the work of Childs and Scharrer.

First published experimental results for gas labyrinth stiffness coefficients are presented in Benckert and Wachter (1979, 1980). Damping coefficients were not obtained since only static pressure measurements of the individual chambers were made. Thieleke and Stetter (1990) as well as Kwanka, et al. (1993), have also carried out similar efforts.

The research summarized in Childs (1993) provided the first measurements of labyrinth seal damping coefficients. While the results gave the first comprehensive basis for comparison against predictions, Childs and Ramsey (1991) revealed the importance of testing at or near the application conditions. The seal test rig was further extended toward this goal by Childs and Scharrer (1986a) and then again by Elrod, et al. (1995).

Wagner and Steff (1996) further expanded the existing experimental knowledge database to geometries and gas conditions matching industrial applications, namely, pressure differential, size, and speed. Pressures of 70 bar (1015 psi) were possible at surface speeds of up to 157 m/s (515 f/s).

The main objective of this paper is to examine the stability results for several industrial representative centrifugal compressors. The API Level I modified Alford's cross-coupling force calculation is examined to determine if it is indeed a conservative estimation of the compressors destabilizing forces by comparing it to the API Level II labyrinth seal calculated forces based on Kirk (1988a, 1988b, 1990). Also, specifics of the labyrinth analysis are examined to determine what parameters are key in determining centrifugal compressor stability. Some of the parameters examined include bearing clearance tolerance range, labyrinth seal clearance, and labyrinth seal inlet swirl effects.

THE KAYBOB INSTABILITY

As a historical perspective, a brief summary of the Kaybob instability will be presented (Smith, 1975; Fowlie and Miles, 1975). This nine-stage low-pressure natural gas injection compressor was commissioned in 1971 in Alberta, Canada. Key operating parameters are summarized in Table 1. The maximum continuous speed (MCS) is 11,400 rpm with 18 MW gas at 1150 psi inlet and 3175 psi discharge. The bearing span, L_b, to midshaft diameter, D_{ms}, ratio is 13.2, indicating a very flexible shaft. The compressor's cross section is shown in Figure 1.

Table 1. Example Centrifugal Compressor Design Data.

Parameter	Kaybob	Example #1	Example #2	Example #3	Example #4	Example #5
Type	Injection	Hydrogen	Propane Refrigeration	Injection #1	Injection #2	Mixed Refrigeration
# Stages	9	10	3	4	4	5
Configuration	Back-Back	Straight	Straight	Straight	Straight	Straight
Speed (rpm)	11,400	10,750	3,000	12,700	9,900	3,000
Rotor Weight (lbm)	-	1,340	36,689	540	422	44,730
Horse Power (hp)	-	12,000	65,000	30,000	11,000	93,000
P_{in} (psi)	1,150	800	20	1,200	5,600	60
P_{disch} (psi)	3,175	1,725	100	3,300	9,000	320
Mole Weight	18	6	44	17	25	25
Bearing Span (in)	59.7	65	230	59.3	47.8	222
D_{ms} (in)	4.5	5.75	22.4	6.69	6.59	21.8
L_b/D_{ms}	13.2	11.3	10.3	8.86	7.26	10.2
Bearings	5 Pad Tilt	5 Pad Tilt	5 Pad Tilt	4 Pad Tilt	5 Pad Tilt	5 Pad Tilt
Seals	Oil	Dry Gas	Dry Gas	Dry Gas	Dry Gas	Dry Gas
Balance Piston	Tooth Laby	Honeycomb	Tooth Laby	Tooth Laby	Tooth Laby	Tooth Laby
Alford's Q_a (lbf/in)	-	57,250	23,046	68,015	72,854	41,907

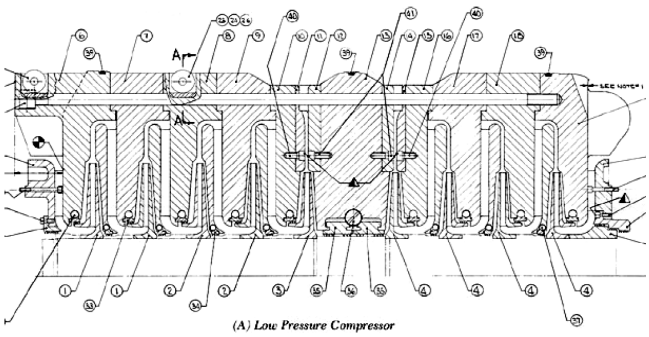

Figure 1. Kaybob Injection Compressor. (Courtesy, Smith, 1975)

The severity of the instability may be seen in the orbit of Figure 2. Note that the outline of the five pad tilting pad bearing is clearly evident in the 6.0 by 9.0 mils peak-to-peak orbit. From Figure 3, the 6.3 mil instability is obviously subsynchronous, reexciting the compressors first critical speed.

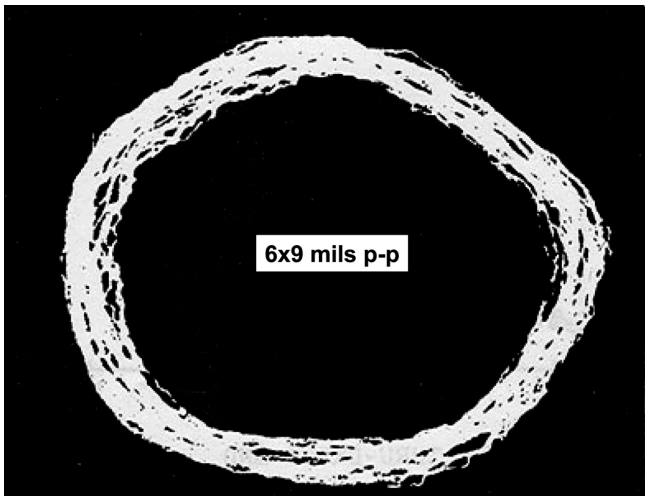

Figure 2. Kaybob Instability Orbit. (Courtesy, Smith, 1975)

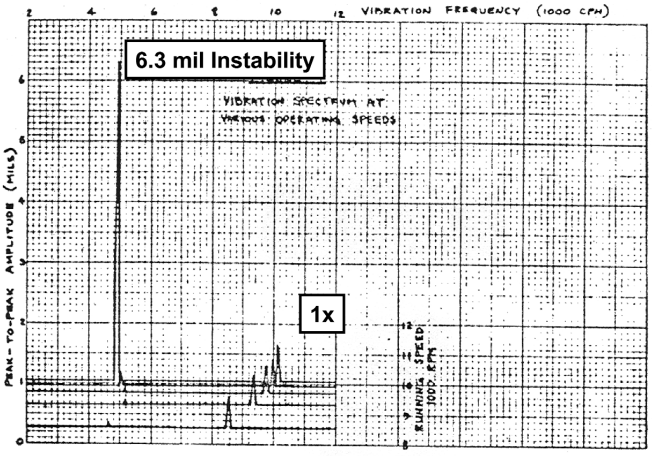

Figure 3. Kaybob Instability. (Courtesy, Fowlie and Miles, 1975)

Attempts to eliminate the instability included bearing redesigns, oil seal modifications, labyrinth seal modifications, balance piston modifications, a vaneless diffuser retrofit, a squeeze film damper retrofit, and, finally, at least two rotor redesigns (Figure 4). The second rotor redesign included increasing the midshaft diameter. Initially, existing impeller forgings were used, cutting and welding the impeller hub to increase the impeller inside diameter to accommodate the increase in shaft diameter (Figure 5).

Clearly, this effort was extremely costly and time consuming. However, it was instrumental, along with the Ekofisk instability, in providing motivation for improved analytical capabilities, ultimately resulting in the existing stability and labyrinth seal codes as well as the new API stability specification.

LOGARITHMIC DECREMENT

The key parameter in stability analyses and the API stability acceptance criteria is the logarithmic decrement or log dec. The log dec is a measure of the rate of decay of free oscillation and is a convenient way to determine the amount of damping present in the system. Greater damping values produce faster decay rates and more stable systems.

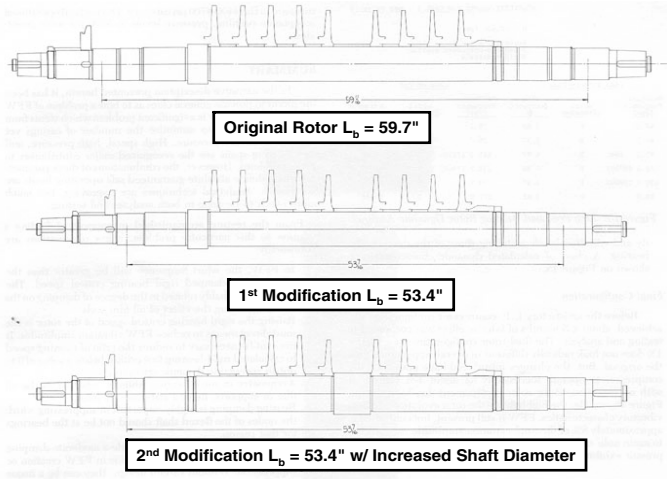

Figure 4. Kaybob Rotor Modifications. (Courtesy, Smith, 1975)

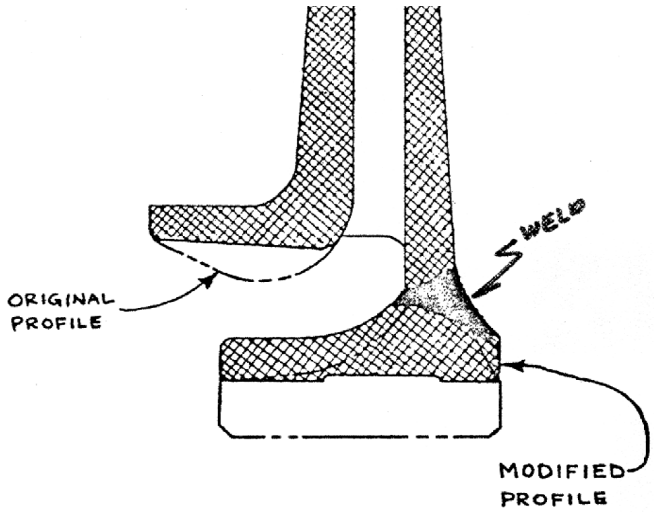

Figure 5. Kaybob Impeller Modification. (Courtesy, Fowlie and Miles, 1975)

The log dec is defined as the natural logarithm of the ratio of any two successive amplitudes. Referring to Figure 6, the log dec is defined as:

$$\delta = \ln\left(\frac{X_1}{X_2}\right) \tag{1}$$

For stable systems, with a positive rate of decay, the log dec is positive. For unstable systems with a negative rate of decay, the log dec is negative. Stable systems with positive log dec values contain sufficient damping to overcome an initial excitation. The resulting displacements will dissipate over time. Conversely, unstable systems with negative log dec values do not contain sufficient damping to overcome the excitation, resulting in increasing displacements over time.

The log dec can also be related to the real, s, and imaginary, ω_d, parts of the eigenvalue as:

$$\delta = -\frac{2\pi \cdot s}{\omega_d} \tag{2a}$$

$$\delta = -\frac{60 \cdot s}{N_d} \tag{2b}$$

where ω_d and N_d are the damped natural frequency in rad/sec and rpm, respectively.

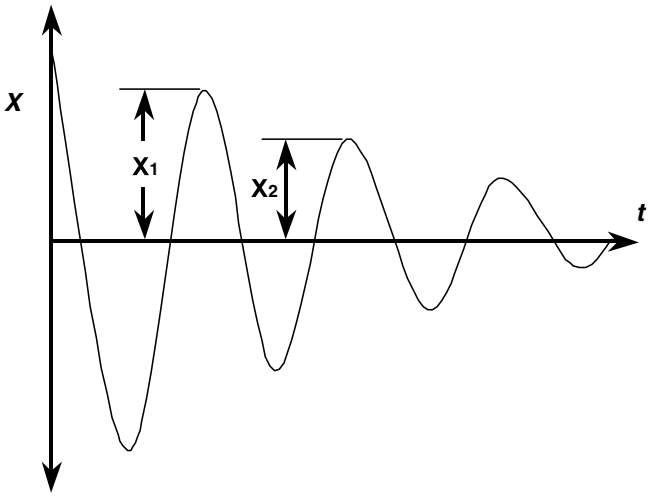

Figure 6. Stable Vibration Wave Form.

EXAMPLE #1— 12,000 HP, 10 STAGE HYDROGEN COMPRESSOR

The first example is a 10 stage 12,000 hp hydrogen centrifugal compressor with a 65 inch bearing span and a L_b/D_{ms} = 11.3. The rotor weighs 1340 lbm and operates at an MCS of 10,750 rpm with dry gas seals and five pad tilting pad journal bearings (Table 1). The inlet pressure is 800 psi with a 1725 psi discharge pressure and a gas mole weight of 6.0. Base log dec values with zero aerodynamic cross-coupling, Q, are 0.26 and 0.40 for minimum and maximum bearing clearances, respectively.

From API Specification 617, Seventh Edition (2002), the modified Alford's equation is:

$$Q = \frac{\beta_c(63{,}000)hp}{H_c(D_c)N}(\rho_{ratio}) \tag{3}$$

where:
β_c = 3.0
hp = 12,000 hp (total all stages)
H_c = Varies stage-to-stage
D_c = Varies stage-to-stage
N = 10,750 rpm
ρ_{ratio} = 1.5 (total across compressor)

Q is calculated for each stage using the above values. Since the stage density ratio and horsepower were not available, the stage horsepower was assumed to be one-tenth of the total value shown above. The stage density ratio was assumed to be the total density ratio shown above, raised to the power of 1/10. The impeller discharge width and impeller diameter are stage-to-stage variables. The summation of all 10 Q values is the API Alford calculated or anticipated cross-coupling value of Q_a = 57,250 lbf/in. With Q_a lumped at the rotor midspan, the resulting log dec values are −0.40 and −0.23 for minimum and maximum bearing clearances, respectively. The API stability acceptance criterion is a log dec greater than 0.1. Thus, a Level II analysis is required.

Prior to any analysis, it had already been decided to use a honeycomb seal on the balance piston. Thus, the stability results reported above include the honeycomb seal dynamic properties (Scharrer and Pelletti, 1994).

With the labyrinth seal geometry, stage gas properties, and stage pressures used as input, a labyrinth seal analysis (Kirk, 1990), is conducted for each of the 10 impeller eye seals. A gas swirl value at the seal inlet is assumed to be 0.6 (60 percent of rotational speed). To be conservative, minimum eye seal clearances are used considering the machining tolerance range for the seal and the seal sleeve. The resulting total labyrinth calculated Q for all 10 eye seals is 15,700 lbf/in.

The shaft seals, with a much lower pressure drop, are neglected. Additionally, the seal flow enters the seal from a stationary part. Thus, the inlet swirl value is low compared to the eye seal swirl (Figure 7). High inlet swirl results in high Q values.

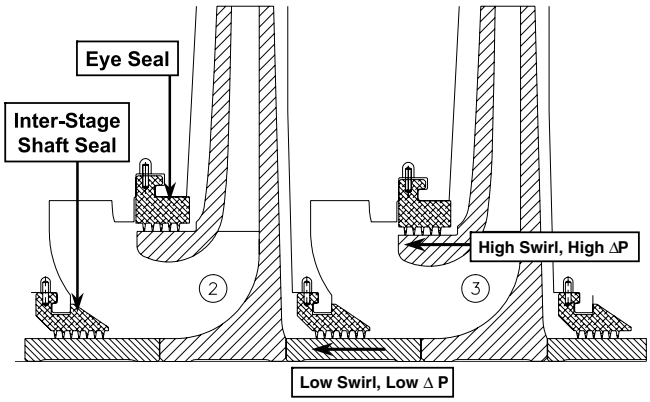

Figure 7. Centrifugal Compressor Labyrinth Seals.

With the total eye seal Q lumped at the rotor center to be conservative, the resulting log dec values are 0.08 and 0.28 for minimum and maximum bearing clearances, respectively.

Instead of estimating the labyrinth eye seal inlet swirl, it can be calculated by modeling the gap between the impeller face and the stator as in Figure 8 (Kirk, 1990). With the inclusion of impeller gap modeling, the inlet swirl is calculated at 0.52 with a resulting Q value for all eye seals of 7600 lbf/in. With this total eye seal Q lumped at the rotor center, the resulting log dec values are 0.17 and 0.35 for minimum and maximum bearing clearances, respectively. As with the Level I analysis, the API stability acceptance criterion for Level II is a log dec greater than 0.1. Thus, this compressor passes API over the bearing clearance tolerance range.

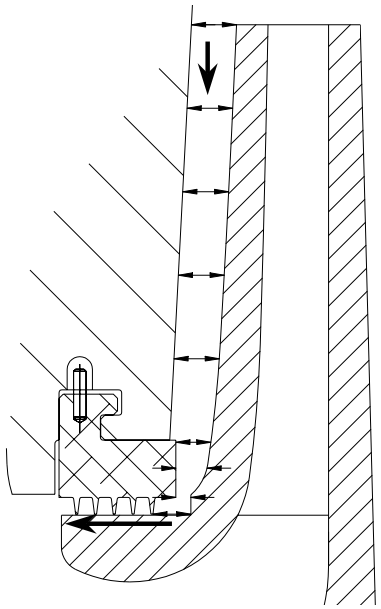

Figure 8. Labyrinth Seal Modeling for Inlet Swirl Calculation.

These results are summarized in Table 2 and shown in Figures 9 and 10 for minimum and maximum bearing clearances, respectively. Also of note from Figures 9 and 10 are the Q values for zero log dec, Q_0. These are 22,500 and 40,000 lbf/in for minimum and maximum bearing clearances, respectively. Clearly for this application, the predicted stability levels using the modified Alford's force is conservative.

Table 2. Hydrogen Compressor Stability Summary.

Bearing Clearance	Q (lbf/in)	Q Description	β_c	Eye Seal Inlet Swirl	N_d (cpm)	Log Dec, δ
Minimum	0	Base	-	-	3,545	0.26
Minimum	57,250	Q_a, Alford	3.0	-	3,590	-0.40
Minimum	15,700	Laby Analysis	-	0.60 Estimated	3,551	0.08
Minimum	7,600	Laby Analysis	-	0.52 Calculated	3,547	0.17
Minimum	22,500	Q_0 (Q for Log Dec = 0)	-	-	3,558	0.00
Maximum	0	Base	-	-	3,361	0.40
Maximum	57,250	Q_a, Alford	3.0	-	3,321	-0.23
Maximum	15,700	Laby Analysis	-	0.60 Estimated	3,333	0.28
Maximum	7,600	Laby Analysis	-	0.52 Calculated	3,348	0.35
Maximum	40,000	Q_0 (Q for Log Dec = 0)	-	-	3,318	0.00

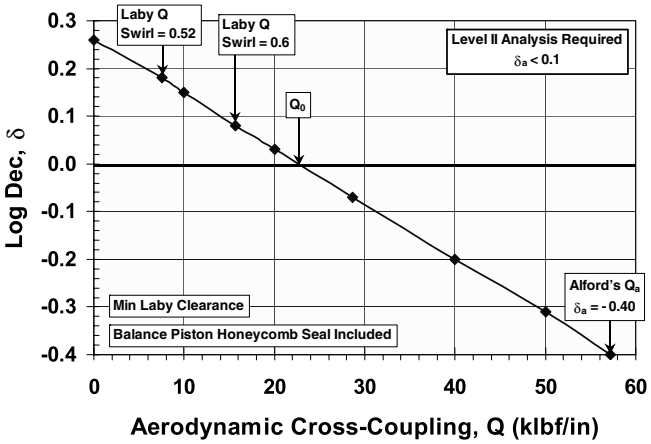

Figure 9. Hydrogen Compressor Stability—Minimum Bearing Clearance.

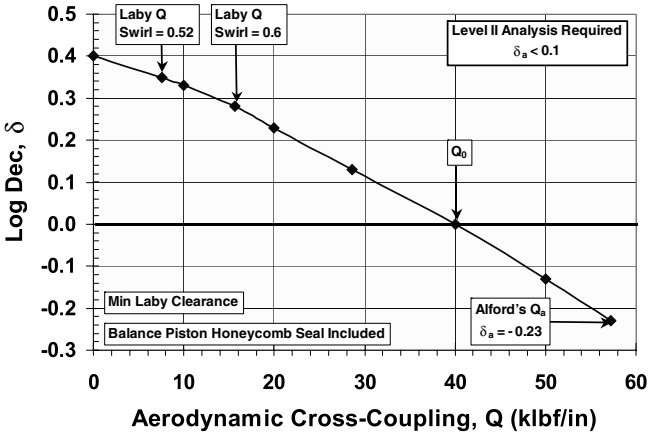

Figure 10. Hydrogen Compressor Stability—Maximum Bearing Clearance.

Eye Seal Inlet Swirl Effects

The effect of inlet swirl on total eye seal Q is shown in Figure 11. The corresponding effect on stability is presented in Figure 12. Note that the inclusion of swirl brakes (Childs and Ramsey, 1991; Moore and Hill, 2000), on the eye seals with an estimated inlet swirl value of 0.3 increases the log dec to 0.28 for minimum bearing and eye seal clearances.

Eye Seal Clearance Effects

The effect of the seal clearance on total eye seal Q is shown in Figure 13. The machining tolerance range is 16 to 20 mils diametral. Assuming that the minimum eye seal clearance decreases by 4 mils diametral due to centrifugal expansion of the impeller, the minimum operating clearance of 12 mils diametral is also shown on Figure 13. The corresponding effect on stability for an inlet swirl of 0.6 and minimum bearing clearance is presented in Figure 14.

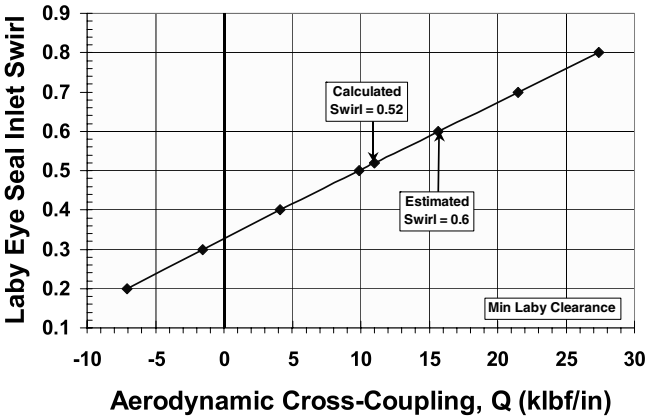

Figure 11. Hydrogen Compressor Q Versus Laby Eye Seal Inlet Swirl.

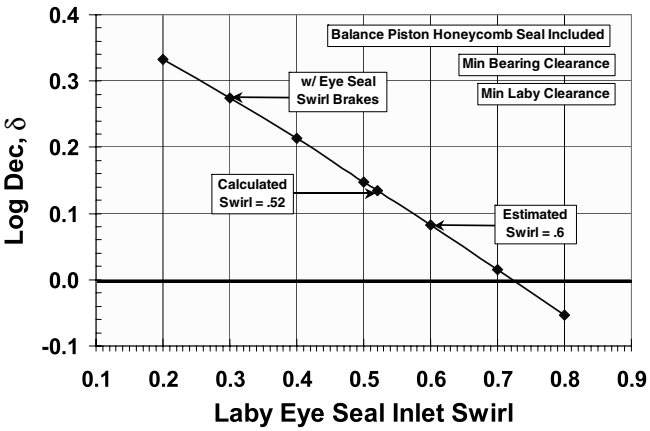

Figure 12. Hydrogen Compressor Stability Versus Laby Eye Seal Inlet Swirl.

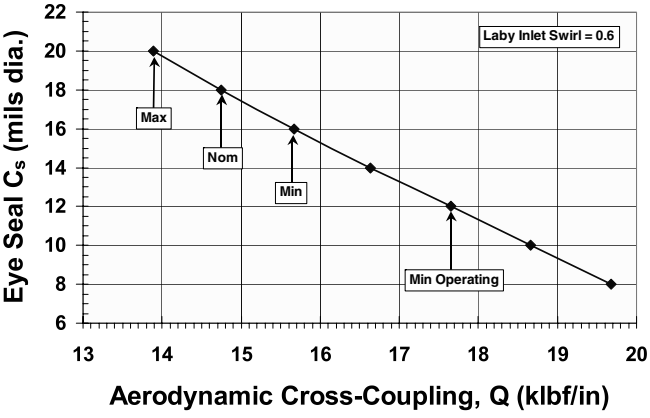

Figure 13. Hydrogen Compressor Q Versus Laby Eye Seal Clearance.

The effects on stability of converging and diverging eye seal clearances are illustrated in Figure 15. Assuming a constant clearance distribution for all eye seal teeth of 12 mils diametral, the resulting log dec is 0.6. If the clearance converges from seal inlet (16.0 mils diametral) to seal discharge (8.0 mils diametral), the log dec decreases to −0.11. Conversely, a divergent clearance from inlet (8.0 mils diametral) to discharge (16.0 mils diametral) produces a log dec of 0.23. These values assume minimum bearing clearance and an inlet swirl value of 0.6.

Clearly, a divergent clearance distribution is preferable for improved stability. While the eye seal principal stiffness is negative

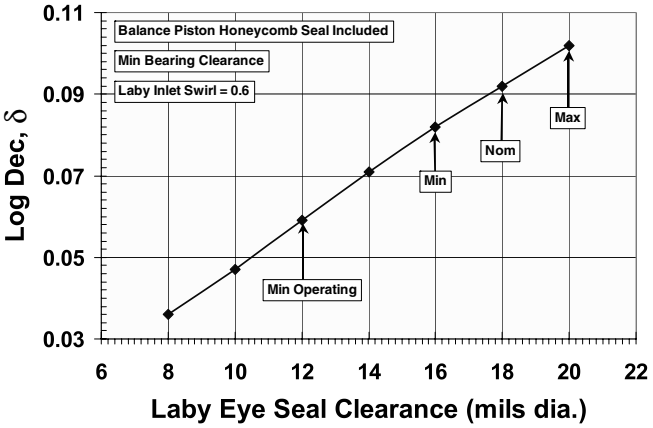

Figure 14. Hydrogen Compressor Stability Versus Laby Eye Seal Clearance.

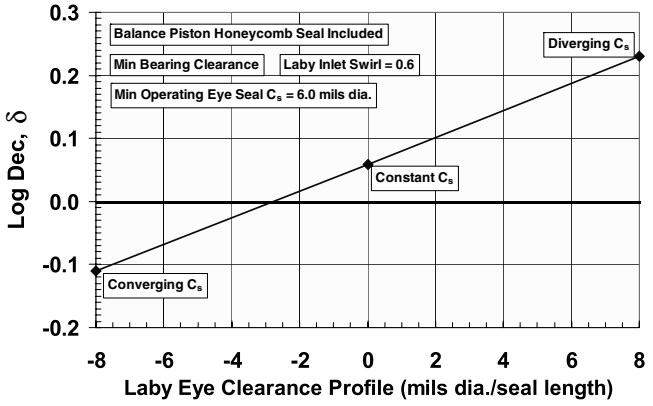

Figure 15. Hydrogen Compressor Stability—Effect of Clearance Profile.

for a diverging clearance, this effect is minimal. Also, the leakage actually decreases for the diverging clearance case compared to a constant clearance. For this compressor, the impeller growth with speed increases from the eye seal discharge location (impeller eye) to the eye seal inlet location resulting in a divergent seal clearance.

Balance Piston Honeycomb Seal— Cell Clogging and Inlet Swirl Effects

One problem with honeycomb seals is that the honeycomb cells may clog or fill with debris. Other nonlabyrinth type seals are also known to clog, such as hole pattern seals. Hole pattern seal test results with plugged holes may be found in Moore and Soulas (2003).

This clogged cell effect for honeycomb seals is illustrated in Figure 16 for minimum bearing clearance and three different honeycomb seal inlet swirl values: 0.8, a pessimistic value; 0.6, a more realistic value; and 0.3, simulating the inclusion of a swirl brake. The plot shows that as the honeycomb cells fill or clog, stability decreases. For the 0.6 inlet swirl case, as long as there are less than 48 percent of the cells filled, the log dec is greater than 0.1, the API acceptance value. For inclusion of a swirl brake (0.3 inlet swirl), the log dec is greater than 0.1 as long as there are less than 60 percent filled cells.

EXAMPLE #2— 65,000 HP, 3 STAGE PROPANE REFRIGERATION COMPRESSOR

The second example is a three stage, three section 65,000 hp propane compressor in a refrigeration service with a 230 inch

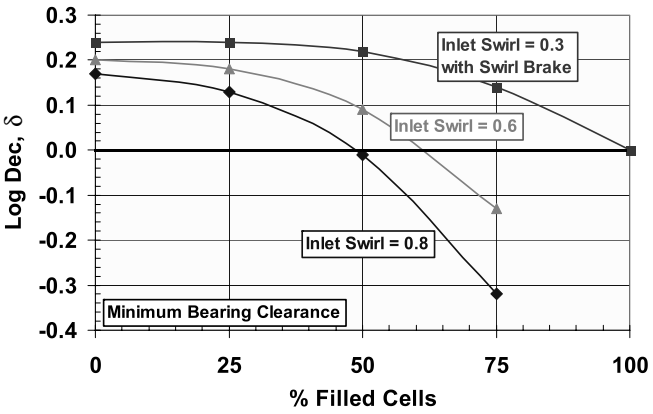

Figure 16. Hydrogen Compressor Stability Versus Percent Filled Balance Piston Honeycomb Cells.

bearing span and a L_b/D_{ms} = 10.3. The rotor weighs in excess of 36,000 lbm and operates at 3000 rpm with dry gas seals and five pad tilting pad journal bearings (Table 1). The inlet pressure is 20 psi with a 100 psi discharge pressure and a gas mole weight of 44. Low base log dec and relatively small destabilizing forces characterize large refrigeration compressors. This machine is no exception. The base log dec (rotor and bearings only, Q = 0.0) of this compressor ranges from 0.18 to 0.13 for the range of bearing tolerances.

In the past, questions have arisen concerning the applicability of "Wachel" type equations (Wachel and von Nimitz, 1981) for compressors with multiple process sections. The concerns have been addressed, for the most part, by applying the modified Alford's equation on a stage by stage basis. In this application, each stage represents a process section with side streams added to the main flow prior to the second and third impellers. Figure 17 presents the rotordynamic model of the compressor.

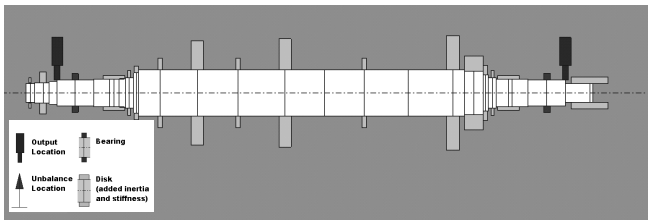

Figure 17. Propane Compressor Cross Section.

Applying Equation (3) to this service, the anticipated destabilizing force, Q_a, can be calculated. On a per wheel basis, the total anticipated destabilizing force is found to be Q_a = 23,046 lbf/in. Applying this to the rotor center yields a log dec of 0.15 and 0.09 for minimum and maximum stiffness bearings, respectively. The stability sensitivity plot is shown on Figure 18. (The tolerance range for the bearing clearances and oil inlet temperatures defines the range of bearing stiffness.) As required by API since the worst case δ_a<0.1, a Level II analysis was performed using the method developed by Kirk (1990) to predict the behavior of the impeller labyrinth seals and balance piston. These destabilizing forces are applied at the physical location of the seal. For the same range of bearing stiffness, the log dec is calculated for the following conditions:

- Rotor and bearing only
- Rotor, bearing, and impeller labyrinth seals
- Rotor, bearing, impeller labyrinth seals, and balance piston

Table 3 contains the results of the Level II analysis and the estimation of rotor stability using the modified Alford's force. As

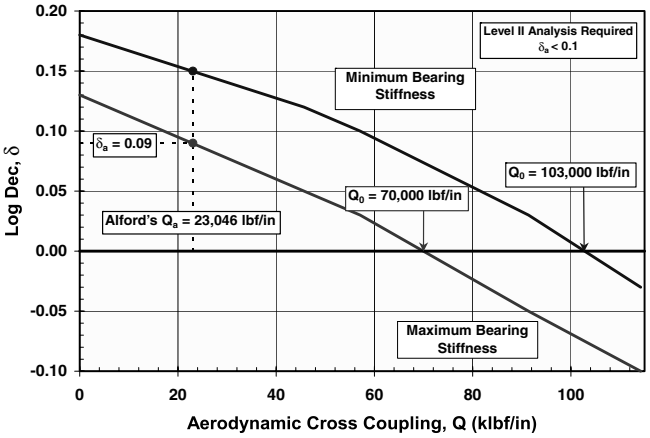

Figure 18. Propane Compressor Stability.

expected, the excitation force due to the labyrinth seals (including the balance piston) is small and has a minor impact on the rotor stability. For this application, the predicted stability levels using the modified Alford's force are conservative.

Table 3. Propane Refrigeration, Injection #1, and Injection #2 Compressor Stability Summary.

Configuration	Bearing Stiffness	Predicted Log Dec, δ		
		Example #2	Example #3	Example #4
		Propane Refrigeration	Injection #1	Injection #2
Rotor / Bearing (Base log dec)				
	Minimum	0.18	1.55	0.84
	Maximum	0.13	0.86	0.39
+ Alford's Qa				
	Minimum	0.15	0.82	*0.52*
	Maximum	0.09	0.24	0.10
+ Laby Seals				
	Minimum	0.17	1.25	0.72
	Maximum	0.12	0.65	0.30
+Laby Seals & Balance Piston				
	Minimum	0.17	1.00	0.38
	Maximum	0.12	0.48	0.12

EXAMPLE #3— 30,000 HP, 4 STAGE INJECTION COMPRESSOR

The third example is a four stage 30,000 hp centrifugal compressor in an injection service with a 59 inch bearing span and a L_b/D_{ms} = 8.86. The rotor weighs 540 lbm and operates at 12,700 rpm with dry gas seals and four pad tilting pad journal bearings (Table 1). The inlet pressure is 1200 psi with a 3300 psi discharge pressure on natural gas. In terms of injection service, this compressor would be considered near the lower end of the discharge pressure range. However, the high horsepower per rotor weight would place it near the top of that range. Recognizing this fact, the manufacturer conservatively designed the compressor with a larger central shaft section (Figure 19). The stiffer shaft produces bending modes with higher relative bearing motion as compared to the shaft center for the first mode. This permits the bearing damping to be more effective in controlling the shaft center and results in higher log dec values.

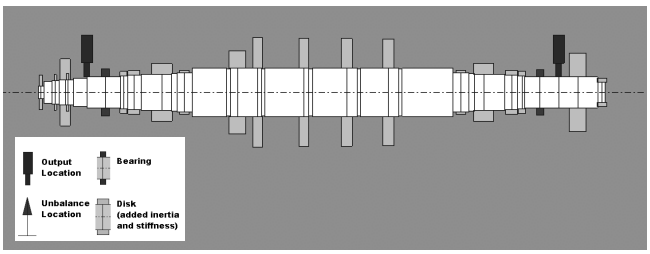

Figure 19. Injection #1 Compressor Cross Section.

As in the prior examples, the Level I analysis is compared against the Level II analysis to determine conservatism. (Note: A Level II analysis is required since Q_0<2*Q_a.) The modified Alford's force is calculated to be 68,015 lbf/in reflecting the high horsepower of the application (Figure 20). Table 3 contains the results of the stability analysis for the same conditions as in example 2. For applications in the midrange of pressure, the balance piston effect on rotor stability is typically equivalent to the impeller eye seals if both are labyrinth type with no antiswirl features. This can be seen for this compressor as the decrease in log dec produced by the impeller labyrinth seals is nearly equal to that produced by including the balance piston. As before, the stability level predicted using the modified Alford's force is conservative in relation to the Level II analysis performed.

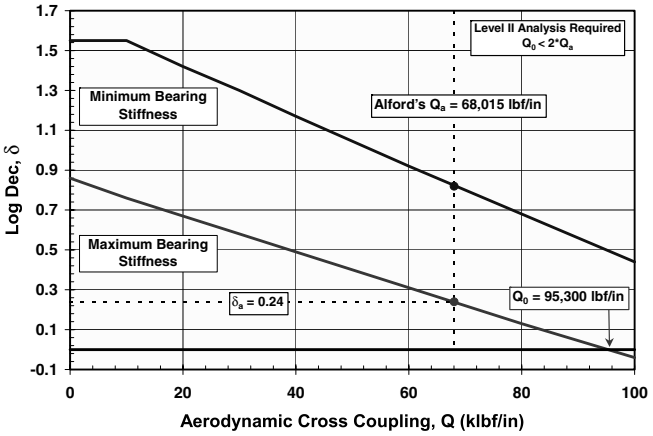

Figure 20. Injection #1 Compressor Stability.

EXAMPLE #4— 11,000 HP, 4 STAGE INJECTION COMPRESSOR

The fourth example is a four stage 11,000 hp centrifugal compressor in an injection service with a 48 inch bearing span and a L_b/D_{ms} = 7.26. The rotor weighs 422 lbm and operates at 9900 rpm with dry gas seals and five pad tilting pad journal bearings (Table 1). The inlet pressure is 5600 psi with a 9000 psi discharge pressure on natural gas. In terms of injection service, this compressor would be considered near the higher end of the discharge pressure range and in the midrange of horsepower per weight ratio. In this application, destabilizing forces are expected to be higher due to the elevated gas densities in the compressor. In fact, a Level II analysis is required due to the average gas density of 115 kg/m^3. As before, the manufacturer conservatively designed the compressor with a larger central shaft section to counter the expected higher destabilizing forces (Figure 21).

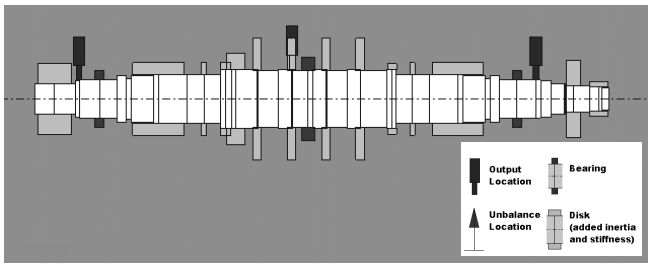

Figure 21. Injection #2 Compressor Cross Section.

For this service, the modified Alford's force is calculated to be 72,854 lbf/in, roughly equal to the compressor in example 3 (Figure 22). Higher gas densities offset the higher horsepower of the previous example. Thus, the anticipated level of destabilizing force is roughly the same for the two examples. Table 3 contains the results of the stability analysis for Level I and Level II

analyses. As with the other injection compressor, a Level II analysis was required since $Q_0<2*Q_a$, indicating that an insufficient safety margin exists between the anticipated destabilizing force and the amount needed to drive the system unstable.

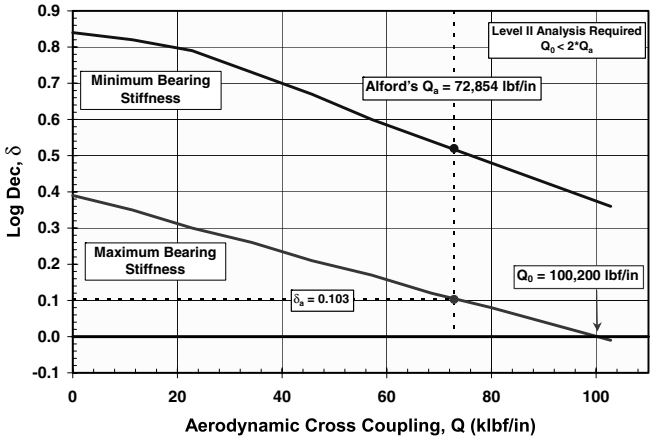

Figure 22. Injection #2 Compressor Stability.

As noted, the Alford's force approximation of the destabilizing force was nearly equal for the two injection compressors. Table 3 confirms this fact when comparing both Level II analyses. The change in log dec from the base value to the condition including all destabilizing forces is roughly −0.55 and −0.40 for the first injection compressor and −0.45 and −0.30 for the second injection compressor for the range of bearing coefficients. This is considered close given the difference in rotor and bearing geometry. Unlike the previous example, the balance piston is producing the majority of the destabilizing force. This was recognized in the early design stages and a shunted balance piston (Kanki, et al., 1988) was employed in the final configuration.

Finally, the Alford's force is shown to be slightly conservative for one bearing condition and somewhat optimistic at the other. However, the conservatism is still seen in the worst case prediction, which would invoke a Level II analysis. Additionally, a Level II analysis was required due to the average gas density in the compressor. This compressor successfully passed a full load test without stability problems.

DISTRIBUTED VERSUS LUMPED ANALYSIS AND EXAMPLE #5—MIXED REFRIGERATION

In the previous three examples, the conservatism of the modified Alford's equation was determined by comparing the resulting log dec values from the Level I and Level II analyses. In this section, a more direct method of comparing an equivalent lumped destabilizing force is presented similar to Memmott (2000). The example 3 injection compressor is used along with a larger refrigeration compressor. The 93,000 hp mixed refrigeration compressor (example 5) has a 222 inch bearing span and a L_b/D_{ms} = 10.2. The two compressors are compared on Figure 23. The rotor weighs 44,730 lbm and operates at 3000 rpm with dry gas seals and five pad tilting pad journal bearings (Table 1). The inlet pressure is 60 psi with a 320 psi discharge pressure using a 25 MW gas.

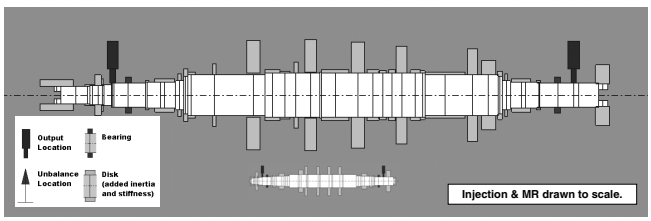

Figure 23. Mixed Refrigerant Compressor Cross Section.

To produce an equivalent destabilizing force as calculated by the modified Alford's equation, an equivalent cross-coupled stiffness is calculated for each seal using the following relation:

$$Q_{eq} = k - C\omega_{cs} \tag{4}$$

The k and C values are determined from a labyrinth seal analysis (Kirk, 1990).

The equivalent modal cross-coupling at the rotor center is defined as:

$$Q_m = \sum M_f Q_{eq} \tag{5}$$

The modal influence factor, M_f, is determined from the normalized mode shape of the first damped natural frequency and represents the displacement at the seal location. The reduced cross-coupling forces are summed for all seal locations. This modal cross-coupling, Q_m, along with the log dec value calculated in the Level II analysis is plotted on the stability sensitivity plots for the two compressor examples at the maximum bearing stiffness only.

Figure 24 presents the results for the first injection compressor, example 3. The minimum modal factor for this compressor was only 0.91 reflecting the stiffer shaft operation of the compressor. Given the labyrinth seal and balance piston forces, the modal cross-coupling was calculated to be 44,933 lbf/in. From Table 3, the Level II log dec including all destabilizing forces was 0.48 at the maximum bearing stiffness. Plotting this point on the sensitivity chart, one finds that the point lies almost directly on the line derived by placing a varying amount of cross-coupling at the rotor center. It needs to be emphasized that the log dec plotted, δ_m, was calculated from the Level II analysis with the seal effects located at the physical location of the seal. From this one can conclude the following:

- The modal reduction produces a reduced cross-coupling force directly comparable to the modified Alford's force.
- The modal cross-coupling also provides an indication of how much margin the rotor has based on the actual seal coefficients. (In this case, the 44,933 lbf/in is compared to the Q_0 amount of 95,300 lbf/in. A safety margin of roughly two exists or more simply the destabilizing effect of the labyrinth seals could be two times larger than calculated before an unstable condition is predicted.)

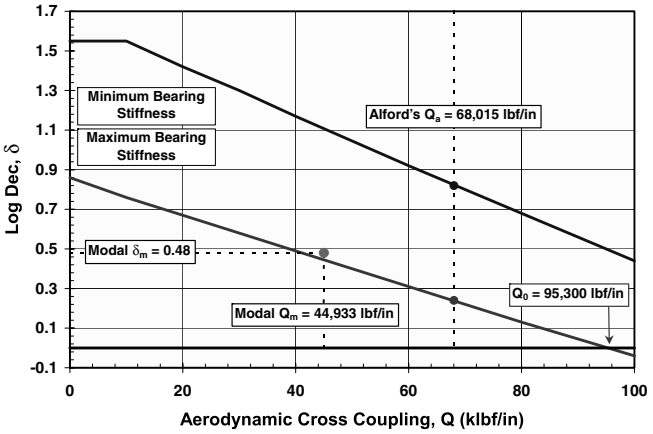

Figure 24. Injection #1 Compressor Stability with Modal Q.

The calculation is repeated for the mixed refrigeration compressor (example 5). For this compressor, the minimum modal factor was 0.56 representing the more flexible bending mode of the shaft. Two configurations of seals are included in the Level II analysis, one with a shunted balance piston and one without a shunt. Both modal cross-couplings and the final Level II log dec values are plotted (Figure 25). As with the injection compressor, both points

lie closely to the sensitivity line from the Level I analysis. This is true even in the case of the shunted balance piston where the net cross-coupling term is negative (or stabilizing).

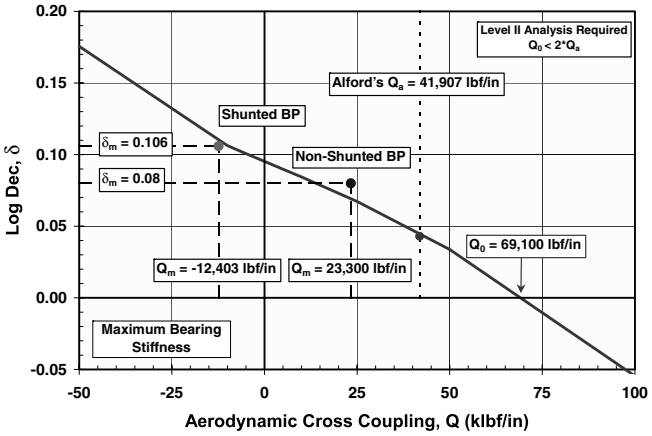

Figure 25. Mixed Refrigerant Compressor Stability with Modal Q.

CONCLUSIONS

The API Level I modified Alford's cross-coupling force calculation was examined and determined to be indeed a conservative estimation of the compressors' destabilizing forces. Several industrial applications were examined including a hydrogen compressor, two high-pressure injection compressors, one with a high horsepower to weight ratio, and two large refrigeration compressors, including a multisection configuration. For all cases, the modified Alford's force was determined to produce the worst case stability level.

Also, specifics of the Level II analysis were examined to determine what parameters are key to determining centrifugal compressor stability. Some well-known influences including bearing clearance tolerance and labyrinth seal inlet swirl were shown to have a major impact on the stability level of the 10 stage hydrogen compressor of example 1. Not so well known was the impact of the labyrinth eye clearance profile. Varying the tooth clearance slope from 8 mils diametral convergent to 8 mils diametral divergent at the impeller eye seals only, changed the predicted log dec from −0.11 to 0.23 for a constant inlet swirl of 0.6. This provides another simple tool to increase the stability of marginal centrifugal compressors.

Finally, a modal approach was presented to permit direct comparison of the Level I and Level II destabilizing forces. Beyond confirming the conservatism of the modified Alford's force, the modal approach also permits use of the stability sensitivity plot to approximate the safety margin of the labyrinth seal coefficients against a zero log dec threshold.

NOMENCLATURE

C_s = Seal diametral clearance (mils)
C = Principle damping (lbf-sec/in)
D_c = Impeller diameter (inch)
D_{ms} = Midshaft diameter (inch)
H_c = Minimum width of the impeller or discharge volute (inch)
hp = Horsepower (hp)
k = Cross-coupled stiffness (lbf/in)
L_b = Bearing span, (inch)
M_f = Modal influence factor
N = Speed (rpm)
N_d = Damped natural frequency (cpm)
P_{disch} = Discharge pressure (psi)
P_{in} = Inlet pressure (psi)
Q = Aerodynamic cross-coupling (lbf/in)
Q_a = Anticipated aerodynamic cross-coupling (lbf/in)
Q_{eq} = Equivalent cross-coupling (lbf/in)
Q_m = Modal cross-coupling (lbf/in)
Q_0 = Aerodynamic cross-coupling for zero log dec (lbf/in)
s = Real part of eigenvalue
$X_{1,2}$ = Amplitude (mils)
β = Efficiency factor
δ = Log dec
δ_a = Log dec for Q_a
δ_m = Final log dec from the Level II analysis
ρ_{ratio} = Density ratio
ω_d = Damped natural frequency (rad/sec)
ω_{cs} = Damped first natural frequency (rad/sec)

REFERENCES

API Standard 617, 2002, "Axial and Centrifugal Compressors and Expander-Compressors for Petroleum, Chemical and Gas Industry Services," Seventh Edition, American Petroleum Institute, Washington, D.C.

API Technical Publication 684, 2005, "Tutorial on Rotordynamics: Lateral Critical Speeds, Unbalance Response, Stability, Train Torsional and Rotor Balancing," Second Edition, American Petroleum Institute, Washington, D.C.

Alford, J. S., 1965, "Protecting Turbomachinery from Self-Excited Rotor Whirl," *ASME Journal of Engineering for Power*, *87*, (4), pp. 333-344.

Bansal, P. N. and Kirk, R. G., 1975, "Stability and Damped Critical Speeds of Rotor-Bearing Systems," *ASME Journal of Engineering for Industry*, Series B, *97*, (4), pp. 1325-1332.

Barrett, L. E., Gunter, E. J., and Allaire, P. E., 1976, "The Stability of Rotor-Bearing Systems Using Linear Transfer Functions—A Manual for Computer Program ROTSTB," Report No. UVA/643092/MAE81/124, School of Engineering and Applied Science, University of Virginia, Charlottesville, Virginia.

Benckert, H. and Wachter, J., 1979, "Investigations on the Mass Flow and the Flow Induced Forces in Contactless Seals of Turbomachines," *Proceedings of the Sixth Conference on Fluid Machinery*, Scientific Society of Mechanical Engineers, Akadémiaki Kikado, Budapest, pp. 57-66.

Benckert, H. and Wachter, J., 1980, "Flow Induced Spring Coefficients of Labyrinth Seals for Application to Rotordynamics," NASA CP-2133, pp. 189-212.

Chen, W. J., 1996, "Instability Threshold and Stability Boundaries of Rotor-Bearing Systems," *ASME Journal of Engineering for Gas Turbines and Power*, *118*, pp. 115-121.

Childs, D. W. and Scharrer, J. K., 1986a, "Experimental Rotordynamic Coefficient Results for Teeth-on-Rotor and Teeth-on-Stator Labyrinth Gas Seals, ASME 86-GT-12.

Childs, D. W. and Scharrer, J. K., 1986b, "An Iwatsubo-Based Solution for Labyrinth Seals: Comparison to Experimental Results," *ASME Journal of Engineering for Gas Turbines and Power*, *108*, (2), pp. 325-331.

Childs, D. W., and Ramsey, C., 1991, "Seal Rotordynamic-Coefficient Test Results for a Model SSME ATD-HPFTP Turbine Interstage Seal With and Without a Swirl Brake," *ASME Journal of Tribology*, *113*, pp. 113-203.

Childs, D. W., 1993, *Turbomachinery Rotordynamics: Phenomena, Modeling, and Analysis*, New York, New York: John Wiley & Sons, Inc.

Edney, S. L., Fox, C. H. J., and Williams, E. J., 1990, "Tapered Timoshenko Finite Elements for Rotor Dynamics Analysis," *Journal of Sound and Vibration*, *137*, (3).

Elrod, D. A., Pelletti, J. M., and Childs, D. W., 1995, "Theory Versus Experiment for the Rotordynamic Coefficients of an

Interlocking Labyrinth Gas Seal," ASME Paper 95-GT-432, Presented at the International Gas Turbine and Aeroengine Congress and Exposition, Houston, Texas.

Fowlie, D. W. and Miles, D. D., 1975, "Vibration Problems with High Pressure Centrifugal Compressors," ASME 75-Pet-28.

Geary, C. H., Damratowski, L. P., and Seyer, C., 1976, "Design and Operation of the World's Highest Pressure Gas Injection Centrifugal Compressor," Paper Number OTC 2485, Presented at the Eighth Annual Offshore Technology Conference, Houston, Texas.

Gunter, E. J., 1966, "Dynamic Stability of Rotor-Bearing Systems," NASA SP-113.

Gunter, E. J., 1967, "The Influence of Internal Friction on the Stability of High Speed Rotors," *ASME Journal of Engineering for Industry*, Series B, *89*, (4), pp. 683-688.

Iwatsubo, T., Matooka, N., and Kawai, R., 1982, "Spring and Damping Coefficients of the Labyrinth Seal," NASA CP-2250, pp. 205-222.

Kanki, H., Katayama, K., Morii, S., Mouri, Y., Umemura, S., Ozawa, U., and Oda, T., 1988, "High Stability Design for New Centrifugal Compressor," *Rotordynamic Instability Problems in High-Performance Turbomachinery*, NASA CP-3026, pp. 445-459.

Kirk, R. G., 1980, "Stability and Damped Critical Speeds: How to Calculate and Interpret the Results," *CAGI Technical Digest*, *12*, (2).

Kirk, R. G., 1988a, "Evaluation of Aerodynamic Instability Mechanisms for Centrifugal Compressors—Part I: Current Theory," *ASME Journal of Vibration, Acoustics, Stress, and Reliability in Design*, *110*, (2), pp. 201-206.

Kirk, R. G., 1988b, "Evaluation of Aerodynamic Instability Mechanisms for Centrifugal Compressors—Part II: Advanced Analysis," *ASME Journal of Vibration, Acoustics, Stress, and Reliability in Design*, *110*, (2), pp. 207-212.

Kirk, R. G., 1990, "A Method for Calculating Labyrinth Seal Inlet Swirl Velocity," *ASME Journal of Vibration and Acoustics*, *112*, (3), pp. 380-383.

Kwanka, K., Ortinger, W., and Steckel, J., 1993, "Calculation and Measurement of the Influence of Flow Parameters on Rotordynamic Coefficients in Labyrinth Seals," *Rotordynamic Instability Problems in High-Performance Turbomachinery*, NASA CP-3239, pp. 209-218.

Lund, J. W., 1965, "Rotor Bearing Dynamics Design Technology, Part V," AFAPL-TR-65-45, Aero Propulsion Laboratory, Wright-Patterson Air Force Base, Dayton, Ohio.

Lund, J. W., 1974, "Stability and Damped Critical Speeds of a Flexible Rotor in Fluid Film Bearings," *ASME Journal of Engineering for Industry*, *96*, (2), pp. 509-517.

Memmott, E. A., 2000, "Empirical Estimation of a Load Related Cross-Coupled Stiffness and the Lateral Stability of Centrifugal Compressors," Presented at the 18th Machinery Dynamics Seminar, Canadian Machinery Vibration Association, Halifax, Nova Scotia, Canada.

Moore, J. J. and Hill, D. L., 2000, "Design of Swirl Brakes for High Pressure Centrifugal Compressors Using CFD Techniques," *Proceedings of the Eighth International Symposium of Transport Phenomena and Dynamics of Rotating Machinery*, (ISROMAC-8), Honolulu, Hawaii, pp. 1124-1132.

Moore, J. J. and Soulas, T., 2003, "Damper Seal Comparison in a High-Pressure Re-Injection Centrifugal Compressor During Full Load, Full-Pressure Factory Testing Using Direct Rotordynamic Stability Measurement," *Proceedings of DETC '03*, ASME Design Engineering Technical Conferences and Computers and Information in Engineering Conference, Chicago, Illinois.

Murphy, B. T. and Vance, J. M., 1983, "An Improved Method for Calculating Critical Speeds and Rotordynamic Stability of Turbomachinery," *ASME Journal of Engineering for Power*, *105*, (3), pp. 591-595.

Nelson, H. D. and McVaugh, J. M., 1975, "The Dynamics of Rotor-Bearing Systems Using Finite Elements," *ASME Journal of Engineering for Industry*, *98*, (2), pp. 593-600.

Ramesh, K. and Kirk, R. G., 1993, "Stability and Response of Rotors Supported on Active Magnetic Bearings," Proceedings of the 14th ASME Vibrations and Noise Conference, DE- 60, *Vibration of Rotating Systems*, pp. 289-296.

Rouch, K. E. and Kao, J. S., 1979, "A Tapered Beam Finite Element for Rotor Dynamics Analysis," *ASME Journal of Sound and Vibration*, *66*, pp. 119-140.

Ruhl, R. L. and Booker, J. F., 1972, "A Finite Element Model for Distributed Parameter Turborotor Systems," *ASME Journal of Engineering for Industry,* Series B, *94*, (1), pp. 126-132.

Scharrer, J. K. and Pelletti J. M., 1994, "Commercial Applications of Space Propulsion Turbomachinery Component Technology," SAE Paper Number 941197, Presented at the SAE International Aerospace Atlantic Conference and Exposition, Dayton, Ohio.

Smith, K. J., 1975, "An Operational History of Fractional Frequency Whirl," *Proceedings of the Fourth Turbomachinery Symposium, Turbomachinery Laboratory*, Texas A&M University, College Station, Texas, pp. 115-125.

Thieleke, G. and Stetter, H., 1990, "Experimental Investigations of Exciting Forces Caused by Flow in Labyrinth Seals," *Rotordynamic Instability Problems in High-Performance Turbomachinery*, NASA CP-3122, pp. 109-134.

Wagner, N. G. and Steff, K., 1996, "Dynamic Labyrinth Coefficients from a High-Pressure Full-Scale Test Rig Using Magnetic Bearings," *Rotordynamic Instability Problems in High-Performance Turbomachinery*, NASA CP-3344, pp. 95-111.

Wachel, J. C. and von Nimitz, W. W., 1981, "Ensuring the Reliability of Offshore Gas Compression Systems," *Journal of Petroleum Technology*, pp. 2252-2260.